

Advanced Feedback Enhances Sensorimotor Adaptation

Tianhe Wang^{1,2,*}, Guy Avraham^{1,2}, Jonathan S. Tsay^{1,2}, Tanvi Thummala³, Richard B. Ivry^{1,2}

1 Department of Psychology, University of California, Berkeley, California;

2 Helen Wills Neuroscience Institute, University of California, Berkeley, California;

3 Department of Molecular and Cell Biology, University of California, Berkeley, California;

Corresponding authors (*):

Tianhe Wang (tianhewang@berkeley.edu)

1 Abstract

2 It is widely recognized that sensorimotor learning is enhanced when the feedback is provided throughout
3 the movement compared to when it is provided at the end of the movement. However, the source of this
4 advantage is unclear: Continuous feedback is more ecological, dynamic, and available earlier than
5 endpoint feedback. Here we assess the relative merits of these factors using a method that allows us to
6 manipulate feedback timing independent of actual hand position. By manipulating the onset time of
7 'endpoint' feedback, we found that adaptation was modulated in a non-monotonic manner, with the peak
8 of the function occurring in advance of the hand reaching the target. Moreover, at this optimal time,
9 learning was of similar magnitude as that observed with continuous feedback. By varying movement
10 duration, we demonstrate that this optimal time occurs at a relatively fixed time after movement onset,
11 an interval we hypothesize corresponds to when the comparison of the sensory prediction and feedback
12 generates the strongest error signal.

13 Introduction

14 Implicit adaptation ensures that the sensorimotor system remains exquisitely calibrated in the face of a
15 variable environment and fluctuations in the internal state of the agent. This process occurs automatically
16 in response to sensory prediction error, the mismatch between the expected sensory consequences of a
17 movement and the actual feedback^{1–3}. A common way to examine constraints on sensorimotor adaptation
18 is to manipulate the visual error. For example, by occluding the arm and providing cursor feedback, a polar
19 transformation (e.g., visuomotor rotation) can be used to introduce a discrepancy between the actual and
20 perceived position of the hand. This discrepancy serves as an error signal that is used to recalibrate the
21 sensorimotor system to minimize future errors when a similar action is produced.

22

23 In studies of visuomotor adaptation, two types of visual feedback are typically used: Continuous feedback
24 where the cursor is visible throughout the movement and thus provides feedback of the movement
25 trajectory, and endpoint feedback where the cursor is only presented when the hand reached its terminal
26 position or at the radial distance of the target (Fig. 1c). It is well-established that adaptation in response
27 to endpoint feedback is attenuated compared to adaptation in response to continuous feedback^{4–6}. This
28 effect is especially pronounced in measures of implicit adaptation, with little difference between online
29 and endpoint feedback on measures reflective of strategic changes in performance⁷. Moreover, the
30 efficacy of endpoint feedback is constrained by timing. Specifically, when the presentation of the feedback
31 cursor is delayed relative to the hand movement, adaptation is markedly attenuated^{8–12}. Indeed, delaying
32 endpoint feedback by just 100ms can produce a dramatic reduction in the magnitude of implicit
33 adaptation^{13,14}.

34

35 At present, it remains unclear why continuous feedback is advantageous relative to endpoint feedback.
36 There are many notable differences between these two modes. First, by definition, continuous feedback

37 is dynamic and endpoint feedback is static. Given the dynamic nature of most human sensorimotor skills,
38 the nervous system may be more responsive to the ecological nature of continuous feedback. Second,
39 continuous feedback provides a continuous stream of spatiotemporal information. Not only does this
40 provide an opportunity to sample the feedback at multiple points of time and space, but the movement
41 of the cursor might be attentionally engaging¹⁵. Third, continuous feedback is provided as soon as the
42 movement is initiated, whereas endpoint feedback is only available when the hand reaches the target.
43 Similar to the attenuation observed with delayed feedback⁸⁻¹³, the inherent delay in endpoint feedback
44 with respect to movement initiation may attenuate adaptation.

45
46 The goal of the present study was to systematically investigate the difference in adaptation to continuous
47 and endpoint feedback, assessing the relative contributions of dynamics, continuity, and onset timing. To
48 isolate implicit adaptation, we employed task-irrelevant clamped feedback¹⁶. In this task, the angular
49 divergence between the feedback and target is fixed, independent of the position (and thus movement)
50 of the participant's hand (Fig. 1b). Participants are fully informed of the feedback manipulation and
51 instructed to ignore the feedback and always reach straight to the target. Despite these instructions, the
52 participant's behavior has all of the hallmarks of implicit adaptation: Across trials, the heading angle of
53 the hand gradually shifts away from the target in the opposite direction of the clamped feedback, and a
54 pronounced aftereffect is observed when the feedback is removed^{16,17}. Participants are not aware of this
55 change in behavior, believing their terminal hand position to be near the target throughout the
56 experiment¹⁸.

57
58 Clamped feedback provides a unique opportunity to manipulate the timing of both continuous and
59 endpoint feedback. Because the feedback is movement-invariant and predetermined, we can manipulate
60 the onset, duration, and offset of the feedback. For example, endpoint feedback can be presented at

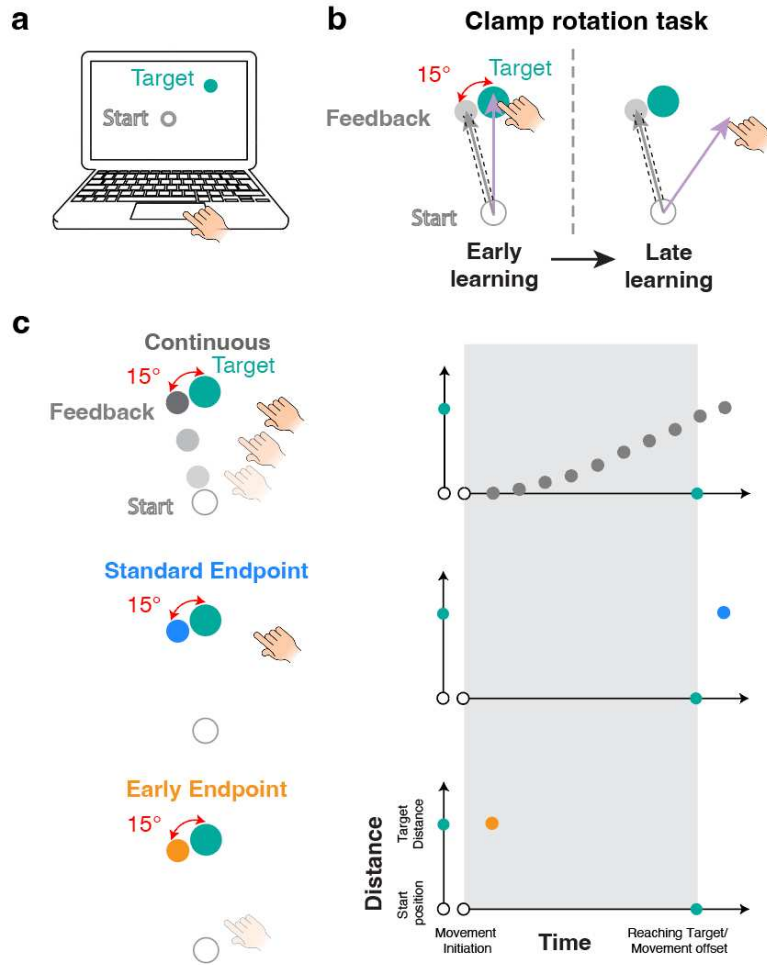
61 movement onset, or even prior to movement onset. Moreover, to examine the influence of temporal
62 continuity, we can manipulate the duration of the feedback to match the endpoint and continuous
63 feedback on this dimension. Through a series of experiments, we manipulate these variables to gain
64 insights into how sensorimotor adaptation is influenced by the spatial-temporal relationship between a
65 movement and its associated feedback.

66

67 Results

68 **Implicit adaptation is influenced by the feedback onset time**

69 In the initial experiments, we used a web-based platform to manipulate the temporal and spatial
70 properties of the feedback in a visuomotor rotation task (Fig. 1a)¹⁹. Using their trackpad, participants were
71 instructed to make center-out ‘reaching’ movements. To elicit implicit sensorimotor adaptation, we used
72 clamped feedback in which the cursor was always rotated from the target location by a fixed angle of 15°
73 (Fig. 1b), and thus, not contingent on the participant’s actual movement direction.



74

75 **Figure 1.** Experimental setup, task, and feedback conditions. **A)** Schematic of the web-based experimental setup,
76 depicting the start location (white circle), the cursor (white dot), and a target (cyan dot). **B)** For task-irrelevant
77 clamped feedback, the angular position of the feedback cursor is rotated by 15° with respect to the target, regardless
78 of the heading direction of the hand. **C)** Three types of clamped feedback are illustrated in task space (left) and as a
79 function showing the position and time of the feedback (right). Each dot represents one refresh cycle on the
80 computer display monitor (16.7ms for most of the monitors). Continuous feedback is presented throughout the
81 movement, following the radial distance of the hand from the start location to the target. Standard-endpoint
82 feedback is presented for one refresh cycle after the hand reaches the target distance (corresponding to the last
83 frame of the continuous feedback condition). Early-endpoint feedback is presented for one refresh cycle at the radial
84 distance of the target when movement initiation is detected. The gray area indicates the interval between
85 movement onset and when the radial distance of the movement reaches the target amplitude. Due to hardware

86 limitations, there is a delay between detection of the hand movement and the onset of the feedback (relevant for
87 continuous and early endpoint feedback), and a delay between when the hand reaches the target amplitude and
88 presentation (relevant for standard endpoint feedback).

89

90 We compared three feedback conditions in Experiment 1a (Fig. 1c). Two of these corresponded to the
91 standard modes of feedback, continuous and endpoint, with the feedback cursor presented throughout
92 the movement for the former and only at the endpoint for the latter. We expected to observe greater
93 adaptation to continuous feedback compared to standard-endpoint feedback, demonstrating that this
94 well-established effect is manifest on our web-based platform. For the third condition, we manipulated
95 the onset time of the endpoint feedback, presenting it at the endpoint position for one refresh cycle as
96 soon as movement initiation was detected. In this way, this early-endpoint feedback is matched to
97 continuous feedback in terms of onset time and to the standard-endpoint feedback in terms of spatial
98 position and temporal duration.

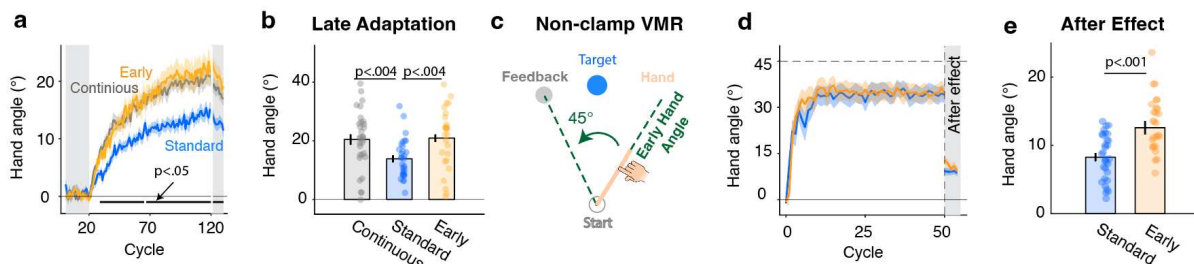
99

100 Following a baseline period with veridical feedback, clamped feedback was presented for 400 trials, with
101 the three modes of feedback tested in different groups of participants. Participants showed robust
102 adaptation in all three conditions (Fig. 2a), with the shift in hand angle persisting across a no-feedback
103 washout block. Consistent with prior studies⁴⁻⁷, participants adapted less in response to standard-
104 endpoint feedback compared to continuous feedback. Surprisingly, early-endpoint feedback resulted in a
105 level of adaptation that was comparable to continuous feedback. Using a non-parametric cluster-based
106 permutation analysis (see Methods), significant differences between conditions were observed across
107 almost the entire extent of the perturbation and washout blocks. Focusing on a pre-specified epoch near
108 the end of the perturbation block, we performed a series of post hoc pairwise comparisons. The hand
109 angle in the standard-endpoint condition was lower than in the continuous ($t(61)=3.2$, $p_{bf}=0.004$,

110 $BF_{10}=16.3$, $d=0.81$) and early-endpoint conditions ($t(57)=3.3$, $p_{bf}=0.004$, $BF_{10}=19.4$, $d=0.85$). No difference
111 was found between the continuous and early-endpoint conditions ($t(56)=0.18$, $p_{bf}=1$, $BF_{10}=0.27$, $d=0.048$).
112 This result provides a striking demonstration of the relevance of feedback onset timing: Providing
113 endpoint feedback as early as continuous feedback, even for just a single refresh cycle, was sufficient to
114 offset the attenuating effects of standard-endpoint feedback.

115

116



117
118 **Figure 2.** Implicit adaptation is enhanced by advancing endpoint feedback. **a**, Experiment 1a: Hand angle time course
119 for the continuous (gray), standard-endpoint (blue), and early-endpoint (yellow) conditions in Experiment 1a. The
120 light gray regions indicate baseline and washout (no feedback) blocks. Black horizontal lines at the bottom indicate
121 clusters showing significant main effects of feedback. **b**, Implicit adaptation magnitude calculated over cycles 110-
122 120 (late adaptation). **c**, Experiment 1d: Illustration of trial in visuomotor rotation task with contingent endpoint
123 feedback; the cursor is rotated by 45° with respect to the projected position of the hand based on actual hand
124 position early in the movement. **d**, Time courses of hand angle, and **e**, implicit adaptation magnitude calculated over
125 the first cycle in the washout block of Experiment 1d. Shaded area in a and d and error bars in b and e represent
126 standard error. Dots in b and e represent individual participants.

127
128 There was a near-significant difference between groups in movement time ($F(2, 88)=2.9$, $p=0.06$,
129 $BF_{10}=0.49$, $\eta_p^2=0.06$) and a significant group difference in reaction time ($F(2, 88)=9.4$, $p<0.001$, $BF_{10}=85.9$,
130 $\eta_p^2=0.17$). Overall, the standard-endpoint group tended to start their movements faster and move slower

131 (Fig. S2). However, this pattern was observed in both the baseline and perturbation blocks, indicating that
132 it was likely due to random variation between the three groups rather than due to the clamped feedback
133 manipulation. Nonetheless, we confirmed that the advantage of continuous and early-endpoint feedback
134 holds even when we regressed out individual differences in median movement duration and median
135 reaction time, as well as age and gender (Table S1).

136

137 The advantage of early-endpoint feedback could occur if participants used the feedback to make mid-
138 movement feedback corrections. For example, seeing the feedback shifted 15° in the clockwise direction
139 might elicit an online correction in the opposite direction, a response that would inflate our estimate of
140 adaptation. In Experiment 1a, our code only saved hand position when the target radial distance was
141 reached, making it impossible to determine if there was evidence for online corrections. To address this
142 concern, we recorded the entire movement trajectory for all three conditions in Experiment 1b. The basic
143 pattern of adaptation was replicated with the early-endpoint and continuous conditions producing
144 comparable levels of adaptation, both higher than that observed in the standard-endpoint condition (Fig.
145 S3). We found no evidence of online corrections in all three feedback conditions, and no difference in
146 reaction time, movement time, and movement speed (Fig. S4).

147

148 The code for the online study was written with the aim of presenting the feedback in the early-endpoint
149 condition immediately after movement initiation. However, the actual presentation time is delayed by
150 two factors: 1) The time to detect movement along the trackpad and 2) the time required to present the
151 visual feedback (Fig. S1). We quantified this delay in the lab by having a few pilot participants perform the
152 task while we made video recordings simultaneously of the participants' hand and monitor with different
153 devices. By this method, we estimated the delay between movement onset and feedback onset (in the
154 early feedback condition) to be between 150-180ms. A previous study showed the delay to present visual

155 feedback on web-based platforms across devices is around 11.5 (± 15.4) ms²⁰; as such, the majority of the
156 delay in our system is likely due to a delay in detecting movement onset from a trackpad. Thus, the early
157 endpoint feedback is likely presented mid-movement rather than at movement onset. We return to this
158 issue in Experiment 3.

159
160 Independent of the delay in movement onset detection, the finding that early-endpoint feedback
161 produces an adaptive response similar to that observed with continuous feedback was surprising. We
162 wondered if this might be the result of a ceiling effect given that implicit adaptation is known to be
163 invariant in response to a large range of errors ($\sim 10^\circ - 90^\circ$)^{16,17,21,22}. To address this question, we
164 compared continuous and early-endpoint feedback in Experiment 1c using a small, 2° visual error clamp.
165 As expected, the asymptote in response to this error was lower than observed in Experiment 1 where the
166 clamp size had been 15°. Importantly, we again did not observe any difference between early-endpoint
167 and continuous feedback ($t(50)=0.93$, $p=0.35$, $BF_{10}=0.40$, $d=0.26$, Fig. S5).

168
169 In Experiment 1d we replaced the visual clamp with position-contingent feedback, addressing the concern
170 that the boost observed with advanced endpoint feedback might be idiosyncratic to the clamp method²³.
171 We used a 45° rotation and compared the early-endpoint and standard-endpoint conditions. It is, of
172 course, not possible in the early endpoint condition to precisely plot the feedback cursor at movement
173 onset based on the (future) endpoint position of the hand. However, given that the movement trajectories
174 are relatively straight, we could predict the endpoint position of the hand based on the heading angle
175 sampled just after movement onset (Fig. 2c). To keep the spatial information similar across conditions, we
176 applied the same method in the standard-endpoint condition (determined angular position of feedback
177 based on the initial heading angle). Adaptation was larger than in experiments 1a-c for both early-
178 endpoint and standard-endpoint conditions (Fig. 2d) as participants followed the instructions to 'make

179 the cursor hit the target.' This behavior likely reflects the composite contributions of both explicit and
180 implicit processes. To estimate implicit adaptation, we focused on the aftereffect, calculated as the mean
181 hand angle in the first cycle of the washout block). Here we again observed greater adaptation in the
182 early-endpoint condition compared to the standard-endpoint condition ($t(56)=3.9$, $p_{bf}<0.001$, $BF_{10}=101.1$,
183 $d=1.0$, Fig. 2e).

184

185 In sum, the results of this first set of experiments demonstrate that advancing the timing of endpoint
186 feedback produces a significant increase in implicit adaptation; indeed, the adaptive response to early
187 endpoint feedback is comparable to that observed in response to continuous feedback. This pattern was
188 observed with feedback signals that varied considerably in terms of error size and movement contingency
189 (clamped or contingent). The absence of evidence of corrective movements suggests that, mechanistically,
190 advancing the onset time of endpoint feedback enhances processes involved in adaptation of a
191 feedforward motor plan rather than processes invoked for online corrections.

192

193 **Temporal and spatial continuity does not influence implicit adaptation**

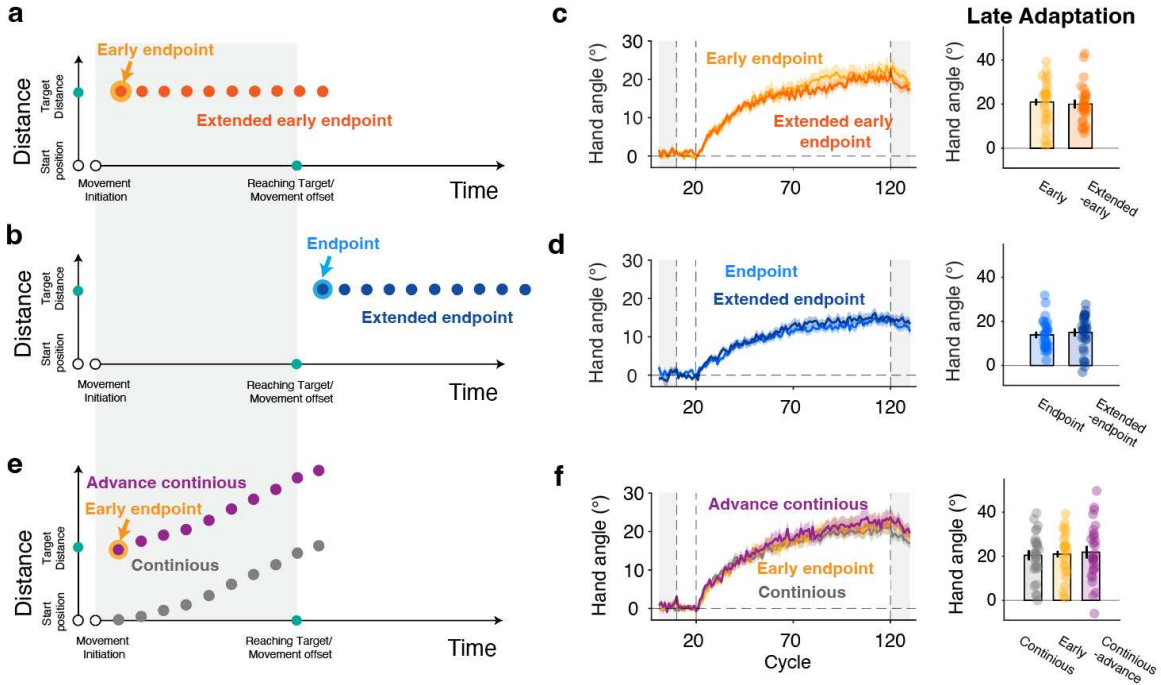
194 Advancing endpoint feedback ensures that feedback onset is matched between continuous and endpoint
195 feedback conditions. However, they still differ in terms of temporal and spatial extent, with continuous
196 feedback available for a longer duration and traversing a larger spatial distance. We next asked if these
197 variables influence implicit adaptation. We examined the influence of temporal continuity in Experiment
198 2a by testing two new conditions. In one condition, we extended the presentation time of the early-
199 endpoint feedback to match it to the duration of the entire movement. In another condition, we extended
200 the duration of the standard endpoint to match the movement time for that trial (on average 84 ms, Fig.
201 3a-b). Thus, in both conditions, the static feedback is visible for the same mean duration as continuous
202 feedback. Compared to the original conditions in Experiment 1 (1 refresh cycle), temporally extending the

203 presentation of endpoint feedback did not influence the time course of adaptation for either the standard-
204 endpoint or early-endpoint conditions (Fig. 3c-d). A regression model showed a significant effect of
205 feedback onset time (coefficient 95% CI: [0.91,9.1], $t(118)=2.4$, $p=0.017$, $BF_{10}=9.4$, $\eta_p^2=0.086$) with no
206 effect of the presentation time duration (coefficient 95% CI: [-5.3,2.8], $t(118)=-0.62$, $p=0.53$, $BF_{10}=0.004$,
207 $\eta_p^2=0.006$).

208

209 To look at the effect of spatial continuity, we created an advanced-continuous feedback condition in
210 Experiment 2b. Here the cursor was presented at the endpoint position upon movement initiation and
211 then moved beyond the target as the participants reached towards the target (Fig. 3e). Thus, the initial
212 position of the feedback is matched to that of the endpoint conditions. This condition resulted in a similar
213 extent of adaptation as standard-continuous in response to both a 15° (Fig. 3f; $t(55)=0.30$, $p=0.77$,
214 $BF_{10}=0.28$, $d=0.079$) and 2° (Fig. S5; $t(42)=-1.3$, $p=0.21$, $BF_{10}=0.58$, $d=-0.4$) visual clamp, surpassing that
215 observed with standard-endpoint feedback. These results are consistent with the hypothesis that the
216 sensorimotor adaptation system is sensitive to the onset time of the feedback but not the temporal or
217 spatial extent of the feedback, two fundamental features of continuous feedback.

218



219
220 **Figure 3. Experiment 2:** Temporal and spatial extent does not influence implicit adaptation. **a-b**, Illustrations of
221 extended versions of early- and standard-endpoint feedback conditions. X-axis indicates time and Y-axis indicates
222 radial distance of the cursor relative to the start position. Each dot represents a refresh cycle. The gray area indicates
223 the movement period. Feedback was presented, on average, for 5 cycles in the extended endpoint conditions. Note
224 that the lighter colors show the timing for the single-cycle variants of early-endpoint and standard-endpoint used in
225 Experiment 1. **c-d**, Left: Time course of hand angle in Experiment 2. The shaded area represents standard error. Light
226 gray areas indicate baseline and washout blocks. No significant clusters were found in the comparison of the brief
227 (1 cycle, data from Experiment 1) and extended versions. Right: Comparison of hand angle measured in late
228 adaptation. **e**, In the advanced continuous condition, the feedback cursor appeared at the endpoint location at
229 movement onset and then moved in the direction of the hand movement. **f**, As in c,d: No significant differences were
230 observed in the cluster-based analysis of the learning functions or during late adaptation.

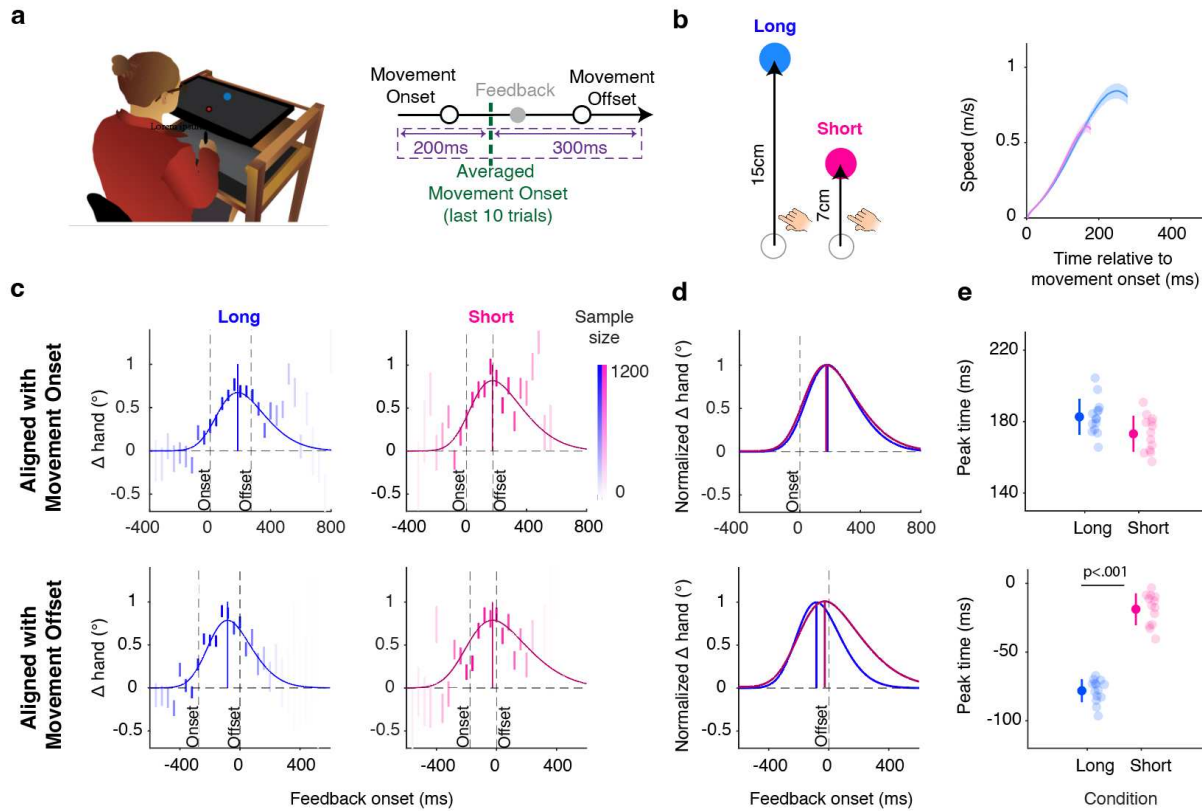
231
232 **The optimal feedback onset time is locked to the movement onset**
233 We next consider two hypotheses that might account for the advantage of early endpoint feedback over
234 standard-endpoint feedback. One hypothesis centers on the idea that optimal adaptation occurs when

235 the error signal is synchronized with the sensory prediction. Considering that 1) the motor command is
236 generated just prior to movement onset, and 2) the sensory prediction is derived from an efference copy
237 of the motor command¹, we assume that the representation of the prediction is strong at a certain time
238 after movement onset. As such, decay in this representation would be minimized when the visual
239 feedback is advanced in time. Alternatively, implicit adaptation may be optimal when the radial position
240 of the visual feedback is subjectively in synchrony with the position of the hand. Given that visual signals
241 are slower than proprioceptive signals²⁴, advancing the visual feedback might be a way to offset this
242 latency difference.

243

244 To evaluate these hypotheses, we turned to a trial-by-trial design in Experiment 3. We used a 15° visual
245 clamp with the direction of the clamp pseudo-randomized to be either clockwise or counterclockwise
246 across trials (and thus prevent accumulated learning). With this design, the index of adaptation is the trial-
247 by-trial change in hand angle²⁵. We varied the onset time of the feedback using intervals that were
248 designed to range from 200 ms prior to movement onset to 300 ms after movement onset. We set this
249 window based on a running average estimate of each participant's mean movement initiation time (Fig.
250 4a). To test whether the optimal feedback time is locked with the movement onset or movement offset,
251 we manipulated movement duration by varying movement distance (7 cm or 15 cm) across participants.
252 The median movement durations for the two conditions were 176.7ms and 272.2ms, respectively (Fig. 4b,
253 Fig. S6). By testing the participants in the lab, all on the same apparatus, we were able to establish precise
254 control over the timing of three critical events -- movement onset, feedback onset, and the time at which
255 the movement reached the target amplitude.

256



257

258 **Figure 4.** The optimal timing of endpoint feedback is associated with the movement onset. **a.** Schematic of the
 259 experimental setup (left) and procedure in the lab for Experiment 3 (right). Feedback time for each trial was
 260 predetermined, selected from a window ranging from -200 ms to +300 ms relative to the average movement onset
 261 time of the last 20 trials. Although participants were instructed to reach through the target ('slicing' movements),
 262 we defined 'movement offset' as the time when the hand reached the target distance. **b,** Left: To vary movement
 263 duration, the required movement amplitude was short or long. Right: The speed profiles for the two movement
 264 amplitudes. Shaded area represents standard error. **c,** Change of hand angle (i.e., Δ hand angle, or trial-by-trial motor
 265 correction) as a function of feedback onset time with respect to the movement onset (top row) or movement offset
 266 (bottom row) for the long and short movements. Each bar is a bin of 40 ms and the darkness of it indicates the
 267 relative number of samples in that bin. Colored curve indicates the best-fitted skewed Gaussian, with the colored
 268 vertical line marking the peak of the function. **d,** Best-fitted skewed Gaussians, normalized to peak height. **e,** Optimal
 269 feedback time relative to the movement onset (top) or offset (bottom), estimated by Jackknife resampling with each

270 dot a sample that included 12 of the 13 participants. The optimal times are statistically indistinguishable for the short
271 and long conditions when determined relative to movement onset, but not when determined relative to movement
272 offset. Error bar represents the standard deviation.

273

274 Feedback onset time had a non-monotonic effect on the trial-by-trial motor correction (Fig. 4c top).
275 Minimal adaptation is observed when the feedback leads movement onset. The function rapidly rises,
276 reaching a peak near movement offset before falling off for longer feedback onset times. The bottom row
277 of Figure 4c plots the same data, but now aligned to the sample at which the hand was detected to be at
278 the target amplitude (referred to as movement offset). For the short movement, the adaptation function
279 peaks close to movement offset. However, for the long movement, the peak is advanced, coming prior to
280 movement offset. Strikingly, adaptation peaked at roughly the same time after movement onset for both
281 the short and long movements.

282

283 The functions in Fig. 4c are based on group-averaged data. It is important to verify that the functions,
284 especially the one showing that the peak occurs in advance of movement offset (e.g., long movement
285 condition), are not distorted due to averaging movement time across trials or participants. To this end,
286 we plotted the motor correction function as a percentage of movement duration on each trial. For
287 example, a 50% feedback onset time corresponds to trials in which the feedback is presented at the
288 midpoint of the movement duration, whereas 100% would indicate trials in which the feedback is
289 presented when the hand reaches the target eccentricity. In this normalized analysis, we observed a
290 similar pattern (Fig. S7). Importantly, the peak of the function for the long movement condition occurs in
291 advance of when the hand reaches the target amplitude, at around 75% of the movement duration.

292

293 To quantify the peak of the feedback function, we used a model-based approach (Fig. 4c). Assuming a
294 skewed Gaussian function, we calculated the time of peak adaptation with respect to movement onset
295 and movement offset, comparing the functions for the short and long movement durations. With respect
296 to movement onset, the functions for the short and long duration movements were very similar (Fig. 4d
297 top), with peaks that were indistinguishable (long: 182.7 ± 9.9 ms, short, 173.2 ± 10.0 ms; $z=0.67$, $p=0.50$,
298 $d=0.19$, Fig. 4e top). In contrast, when we compared the functions for the short and long duration
299 movements aligned with respect to movement offset time, the peaks were markedly different (long: -78.1
300 ± 8.3 ms; short: -18.7 ± 11.5 ms, $z=4.2$, $p<0.001$, $d=1.2$, Fig. 4d-e, bottom).

301
302 Taken together, those results indicate that the optimal time to present feedback does not correspond to
303 the time at which the hand position and feedback position are aligned. Rather, the optimal time for
304 feedback appears to be at a fixed delay relative to movement onset, consistent with the hypothesis that
305 learning is strongest when the feedback is temporally aligned with the sensory prediction.

306

307 Discussion

308 Visual feedback provides an essential source of information to improve motor performance. Continuous
309 feedback helps the driver navigate on a curvy country road; endpoint feedback can aid a basketball player
310 when shooting free throws. While many studies have shown that continuous feedback induces faster
311 learning relative to endpoint feedback⁴⁻⁶, the reason for this benefit has not been clear. Not only does
312 continuous feedback provide extended spatiotemporal information, but its onset is also earlier in the
313 movement. In the present study, we used non-contingent, clamped feedback to examine various factors
314 that might underlie the disadvantage of endpoint feedback. The results show that, whereas the duration
315 and spatial extent of the feedback had no impact on the strength of adaptation, the onset time of the

316 feedback was critical. Advanced ‘endpoint’ feedback, even when limited to a single frame, resulting in
317 adaptation comparable to that observed with continuous feedback.

318

319 These observations are especially surprising given that continuous feedback provides richer information
320 than endpoint feedback. However, various lines of studies indicate that implicit adaptation is relatively
321 insensitive to the quality of the feedback. For example, adaptation is insensitive to the uncertainty of the
322 visual feedback, at least for relatively large errors²², suggesting that the implicit learning system may not
323 be sensitive to the quality or ecological validity of the feedback. This point is further underscored by the
324 very fact that robust adaptation is observed in response to clamped feedback despite participants’
325 awareness of the manipulation. These observations point to a system that is highly modular, automatically
326 using an error signal to make feedforward adjustments to keep the sensorimotor system precisely
327 calibrated. The benefit of continuous feedback may be pronounced in feedback control, enabling online
328 adjustments to ensure that the movement goal is achieved^{26,27}.

329

330 The importance of feedback timing has been highlighted in prior studies of visuomotor adaptation. That
331 body of work has emphasized how delaying endpoint feedback can dramatically attenuate
332 adaptation^{8,9,11,13,28}. Implicit in this work is the assumption that the optimal time for endpoint feedback is
333 at movement offset, that is, when the feedback is temporally and spatially synchronized with the hand
334 ^{13,29}. Because these studies used position-contingent feedback, it was only possible to delay the feedback.
335 Taking advantage of the fact that position-independent, clamped feedback is effective in eliciting
336 adaptation, we were able to temporally advance ‘endpoint’ feedback. The enhancement of learning
337 observed with this method indicates that the advantage of continuous feedback does not rest on its
338 spatiotemporal continuity, and that it is not essential that the position of the feedback be synchronized
339 with the position of the hand.

340

341 Having demonstrated the advantage of early endpoint feedback, we set out to determine the optimal
342 time for the feedback. The clamp method allowed us to parametrically manipulate the onset time of
343 endpoint feedback. Here, we transitioned from a web-based platform to the lab to minimize
344 measurement delays and test a wider range of values ranging from well before the movement onset to
345 beyond movement offset. Moreover, by using two distinct movement durations (by manipulating
346 movement amplitude), we could examine if optimal timing was linked to movement onset or movement
347 offset. We observed non-monotonic functions for both amplitudes. The attenuation for the longest
348 feedback onset latencies provides another demonstration of the cost of delayed feedback. Moreover, the
349 attenuation for the shortest latencies indicates that there is a cost for presenting the feedback too early,
350 including the time of movement initiation.

351

352 The peak of the function (i.e., the optimal timing for feedback) was observed at a midway point, one in
353 which the position of the feedback was in advance of the position of the hand. One hypothesis to account
354 for this effect is based on models of multisensory integration. In this framework, the perceived hand
355 position, the signal essential for computing the error, is an integrated representation based on a variety
356 of inputs, including vision and proprioception³⁰. Temporally, one would expect that the contribution of
357 the visual signal will be strongest when it is synchronized with the proprioceptive signal. In terms of neural
358 responses in the brain, visual inputs are delayed by approximately 50 ms relative to proprioceptive
359 inputs^{24,31,32}. Advancing endpoint visual feedback by this interval could enhance visual-proprioceptive
360 synchronization, and thus boost learning. Importantly, since movement offset is defined by hand position,
361 this hypothesis predicts that the optimal timing of feedback should be constant with respect to movement
362 offset. However, this prediction was not supported by the results. More generally, the brain has likely

363 evolved mechanisms to compensate for inherent differences in transmission delays across sensory
364 modalities, negating the need for temporal synchronization in deriving a multisensory signal³³.

365
366 Whereas the multisensory integration hypothesis focuses on the observed feedback, an alternative
367 hypothesis focuses on how this information is compared to the predicted sensory outcome. The latter is
368 assumed to be generated from an efference copy of the motor command. We hypothesize that the
369 feedback timing function reflects the strength of the representation of the sensory prediction. When
370 considered as a discrete event, the 170 ms delay may reflect the interval between the efference copy and
371 time in which the prediction is available; when considered as a continuous neural process, the
372 representation of the prediction may reach its maximal strength around 170 ms after movement initiation.
373 By either view, we assume this representation will decay after its peak. When feedback is temporally
374 advanced, adaptation is therefore strengthened since the feedback arrives prior to the decay of the
375 sensory prediction. This hypothesis is consistent with the observation that the optimal time was time-
376 locked to movement onset, independent of movement duration.

377
378 Temporal constraints are a prominent feature of cerebellar-dependent learning, including sensorimotor
379 adaptation and eyeblink conditioning³³. In the latter, the animal learns to make a blink in response to an
380 arbitrary stimulus (conditioned stimulus, CS) that is predictive of an aversive event (unconditioned
381 stimulus, US). This form of learning is highly sensitive to the interval between the CS and the US³⁴, showing
382 a non-monotonic function similar to that observed in the present study. Learning is negligible when the
383 US occurs before or together with the onset of the CS, peaks when the CS leads the US by between 200 –
384 400 ms, and decreases for longer intervals^{35–38}. The rise of this function has been assumed to reflect the
385 time required to generate an expectancy of the US and adaptive motor response that will attenuate the
386 aversive effects of the US. The reduced efficacy of learning for longer CS-US intervals is assumed to reflect

387 temporal limitations within the cerebellum for maintaining the sensory prediction. This account of the
388 optimal timing for eyeblink conditioning is similar to our account of optimal timing for visuomotor
389 adaptation. In the latter, the motor commands and visual feedback serve as equivalents for the CS and
390 US, respectively. Consistent with this notion, we have recently shown that when temporal constraints are
391 imposed, two signature phenomena of classical conditioning, differential conditioning and compound
392 conditioning, are observed in visuomotor adaptation³⁹.

393
394 It remains to be seen whether the benefits of advanced timing hold over a broad range of contexts. Our
395 experimental manipulations were limited to relatively simple reaching movements, performed over two
396 movement amplitudes. Future behavioral studies should examine the effect of feedback timing for
397 movements that span a wider range of durations and contexts. Indeed, a recent study suggests that our
398 optimal timing hypothesis could be tested in the absence of movement. By using a Go-NoGo task, Kim et
399 al. observed adaptation in response to clamped feedback even after trials in which the movement was
400 aborted⁴⁰. Presumably, a motor command was generated on the no-go trials, resulting in a sensory
401 prediction that could be compared to the clamped feedback. This task might be ideal for examining
402 feedback timing given that movement kinematics are eliminated on the no-go trials, removing additional
403 and potentially conflicting sources of information (e.g., proprioceptive signals from the moving limb).

404
405 **Conclusions**
406 A core principle featured in motor learning textbooks is that endpoint feedback elicits less learning than
407 continuous feedback^{41,42}. The present results indicate that a major reason for the disadvantage of
408 endpoint feedback is that it becomes available later than continuous feedback; when ‘endpoint’ feedback
409 is temporally advanced, implicit adaptation was enhanced, reaching a level comparable to that observed
410 with continuous feedback. By systematically varying the onset time of ‘endpoint’ feedback, we found that

411 the optimal feedback time was time-locked to movement onset rather than movement offset. We
412 hypothesize that adaptation is optimized when the sensory prediction is at maximal strength for
413 comparison with the sensory feedback in generating an error signal. These results underscore novel
414 temporal constraints underlying cerebellar-dependent sensorimotor learning.

415 **Methods**

416 **Participants**

417 Testing was conducted online for Experiments 1-2 and in the lab for Experiment 3. For online studies, a
418 total of 272 participants (116 female, mean age = 24.5, SD = 4.7) were recruited through the website
419 prolific.co. We recruited 34 participants for each condition based on a power analysis (see Supplementary
420 Methods). After eliminating participants who failed to meet our performance criteria (see below), the
421 analyses were based on data from 239 participants (27-32 for each condition, 93 females, mean age =
422 24.3, SD = 4.5). Based on self-report data from a prescreening questionnaire, all of the participants were
423 right-handed with normal or corrected-to-normal vision. The online participants were paid around \$8/h.
424 For the lab-based experiment, we recruited 26 undergraduate students (15 female, mean age = 21.5, SD
425 = 4.5) from the University of California, Berkeley community. All of the participants were right-handed
426 based on their scores on the Edinburgh handedness test⁴³ and had normal or corrected-to-normal vision.
427 These participants were paid \$15/h. All experimental protocols were approved by the Institutional Review
428 Board at the University of California, Berkeley. Informed consent was obtained from all participants.

429

430 **Web-based experiments**

431 Online experiments (Exp 1-2) were performed using our web-based experimental platform, OnPoint¹⁹.
432 The code was written in JavaScript and presented via Google Chrome, designed to run on any laptop
433 computer. Visual stimuli were presented on the laptop monitor and movements were produced on the
434 trackpad. Data were collected and stored using Google Firebase. The experimental session lasted around
435 40 minutes

436

437 **Procedure**

438 *Experiment 1a*

439 Clamp rotation task. To start each trial, the participant moved the cursor to a white start circle (radius: 1%
440 of the screen height) positioned in the center of the screen. After 500 ms, a blue target circle (radius: 1%
441 of the screen height) appeared with the radial distance set to 40% of the screen size. There were four
442 possible target locations (+/-45°, +/-135°). The participant was instructed to produce a rapid, out-and-
443 back movement, attempting to intersect the target. The target disappeared when the amplitude of the
444 cursor movement reached the target distance. To help guide the participant back to the start location, a
445 white cursor (radius: 0.6% of screen height) appeared when the hand was within 40% of the target
446 distance. If the movement time was >500 ms, the message 'Too Slow' was presented on the screen for
447 500ms.

448

449 We used a visual clamp to elicit implicit sensorimotor adaptation, manipulating feedback onset time,
450 presentation duration, and spatial continuity. Three types of clamp feedback were employed in
451 Experiment 1 (between-subjects). (1) Continuous feedback: The radial location of the cursor was based
452 on the radial extent of the participant's hand and was visible during the whole movement (up to reaching
453 the target distance) but was independent of the angular position of the hand. (2) Standard endpoint
454 feedback: The cursor was presented at the target distance for one refresh cycle (10~20ms depending on
455 the monitor refresh rate, 16.7ms for 60 Hz monitor) after the hand reached the target distance. In this
456 manner, the timing and position of the cursor was the same in this condition as the last frame for the
457 continuous feedback condition. (3) Early-endpoint feedback: The cursor fleshed at the target distance for
458 one cycle when the hand was detected to exit the start circle. Thus, the onset of the feedback cursor is at
459 the same time as the onset time for continuous feedback.

460

461 There was a total of 520 trials in Experiment 1, arranged in four blocks. 1) A no-feedback baseline block
462 (40 trials). 2) A feedback baseline block with veridical continuous feedback (40 trials). 3) A learning block

463 with clamped feedback (400 trials), where the cursor followed a trajectory that was displaced at a fixed
464 angle from the target. Right before the learning block, a set of instructions was presented to describe the
465 clamped feedback. The angle was set to 15° and the direction of the clamp was either clockwise (CW) or
466 counterclockwise (CCW) with respect to the target, counterbalanced across participants. The participant
467 was informed that the cursor would no longer be linked to their movement, but rather would follow a
468 fixed path on all trials. The participant was instructed to always reach directly to the target, ignoring the
469 cursor. To make sure the participant understood the nature of the error clamp, the instructions were
470 repeated. Moreover, after the first 40 trials with clamped feedback, an instruction screen appeared asking
471 the participant to indicate if they were aiming for the target or another location. If the participant
472 indicated they were reaching to another location, the experiment was terminated. 4) A no-feedback
473 washout block (40 trials). Within each block, trials were grouped into cycles of four trials, with each target
474 (+/-45°, +/-135°) appearing once per cycle (order randomized across cycles).

475

476 *Experiment 1b-c*

477 The methods for Experiments 1b and 1c were essentially the same as in Experiment 1a. The only change
478 in Experiment 1b is that the whole movement trajectory was recorded. In Experiment 1c, the clamp size
479 was reduced to 2° and we replaced the standard-endpoint condition with advanced-continuous feedback
480 condition (see Experiment 2 below).

481

482 *Experiment 1d*

483 *Visuomotor rotation task (VMR)*. To confirm that the results obtained in Experiments 1a-c were not
484 idiosyncratic to clamped feedback, we used a standard visuomotor rotation task in Experiment 1d. Here
485 the position of the feedback cursor during the adaptation block was contingent on the participant's hand
486 position. To encourage strategy use, we opted to use a large 45° rotation (CW and CCW counterbalanced

487 across participants), limited the target position to two locations (135°/315°), and instructed participants
488 to 'make the cursor hit the target' ⁴⁴.

489
490 For both endpoint and early-endpoint feedback, the position of the feedback was rotated 45° from the
491 hand angle obtained at the second data point collected after movement initiation. Early-endpoint
492 feedback was presented right after this data point was sampled, while endpoint feedback was presented
493 when the radial position of the hand reached the target distance.

494
495 As in Experiment 1a, there were four blocks: No-feedback baseline (20 trials), feedback baseline (40 trials),
496 adaptation with contingent rotated feedback (200 trials), and no-feedback washout (20 trials). Within
497 each block, the trials were grouped into cycles of four trials, with each of the two target positions
498 presented twice per cycle. Prior to the start of the adaptation block, the instructions described the size
499 and direction of the rotation and emphasized that the participant should adjust their aim to compensate
500 for the perturbation and make the cursor hit the target. Prior to the washout block, the participant was
501 instructed to cease using any aiming strategy and to again reach directly to the target.

502
503 *Experiment 2*
504 We tested three additional feedback conditions in Experiment 2 to examine the effect of dynamics and
505 feedback duration. In Experiment 2a we examined the role of feedback duration, extending the duration
506 of the static feedback to approximate that observed with continuous feedback. In the extended-endpoint
507 condition, the cursor appeared after the hand reached the target distance and remained visible for an
508 interval equal to the movement duration for that trial. In the extended-early-endpoint condition, the
509 cursor appeared at movement onset and remained visible until the hand reached the target distance. In
510 Experiment 2b we examined the effect of advancing continuous feedback. The cursor appeared at the

511 endpoint position as soon as movement initiation was detected and then continued along that ray until
512 the hand reached the target distance. Thus, the position of the cursor was advanced relative to the
513 position of the hand. The procedure was the same as in Experiment 1a and we compared the performance
514 of these three groups to the relevant conditions from Experiment 1a.

515

516 *Experiment 3*

517 Experiment 3 was designed to derive a function describing how feedback timing modulates the strength
518 of adaptation. To ensure the precise timing of the trial events, we conducted this experiment in person,
519 using the same apparatus for each participant. Participants performed a center-out reaching task on a
520 digitizing tablet (Wacom Co., Kazo, Japan) which recorded the motion of a digitizing pen held in the hand.
521 Stimuli were displayed on a 120 Hz, 17-inches monitor (Planar Systems, Hillsboro, OR) that was mounted
522 horizontally above the tablet, obscuring vision of the arm. The experiment was controlled by a Dell
523 OptiPlex 7040 computer (Dell, Round Rock, TX) running on a Windows 7 operating system (Microsoft Co.,
524 Redmond, WA) with custom software coded in MATLAB (The MathWorks, Natick, MA) using Psychtoolbox
525 extensions.

526

527 The start position (radius: 4 mm) was located in the lower quarter of the screen at the midline. To allow
528 the trial-by-trial analysis of adaptation (see below), we used a single target location (radius: 7 mm, fixed
529 at 45°). The radius from the start position to the target location was set to 7 cm for half of the participants
530 and 15 cm for the other half of the participants. This manipulation was included to produce different
531 movement times for the two groups of participants. During the inbound portion of the movement, a white
532 circle was visible at the start position with the radius of the circle indicating the participants' distance from
533 the start position. In this way, participants were guided to the start position without directional feedback
534 of their movement.

535

536 The experiment began with a block of 16 trials in which a cursor (radius: 3 mm) provided continuous
537 feedback. This was followed by an extended block of 1200 trials with clamped feedback. The clamp was
538 offset from the target by 15°, with CW and CWW deviations intermixed within a cycle of 4 trials. By mixing
539 CW and CWW clamps, there is no cumulative effect of adaptation; rather, the dependent variable of
540 adaptation was the trial-by-trial change in hand angle²⁵. Prior to the onset of the clamped feedback block,
541 participants were fully informed of the clamp manipulation and instructed to always move directly
542 towards the target. The onset time of the clamped feedback was randomly sampled from a uniform
543 distribution ranging from -200 to 300 ms relative to a running average of the individual's movement onset
544 time, calculated over the last 20 trials. The clamp was presented as endpoint feedback for two refresh
545 frames (approximately 16 ms). Note that we did not impose any constraint on movement onset time.

546

547 **Data analysis**

548 The initial data analyses were conducted in MATLAB 2020b. Hand angle was calculated as the angular
549 difference between the target and the hand position at the target radius. Positive values indicate hand
550 angles in the opposite direction of the perturbation experienced by that participant, the direction one
551 would expect due to adaptation. For Experiments 1-2, movement initiation is defined as the first sample
552 where the hand surpassed the radius of the start position. For Experiment 3, movement initiation was
553 defined as the first sample in the time series in which sample-to-sample acceleration remained positive
554 for displacements greater than 5 mm⁴⁵. Movement offset was defined as the first sample in the time series
555 in which the radial distance of the hand reached the target distance. Note that we defined movement
556 offset as the time when the radial distance of the movement reached the target distance even though the
557 actual end of the movement was beyond this point (i.e., slicing movement). Trials with a movement
558 duration longer than 500 ms or an error larger than 70° were excluded from the analyses. We excluded

559 the entire data from participants who had less than 70% valid trials (see Supplementary Methods for
560 details).

561

562 For Experiments 1a-c and 2, the data were averaged over cycles (4 trials/cycle). We examined learning at
563 two time points, during the late phase of the adaptation block and during the aftereffect block. Late
564 adaptation was defined as the mean hand angle over the last 10 cycles of the perturbation block, minus
565 the mean of the no-feedback baseline block (to adjust for individual biases in reach direction). Aftereffect
566 was defined as the mean hand angle over the washout block, minus the mean of the no-feedback baseline
567 block. As a continuous measure of adaptation, we used a cluster-based permutation test (Arnal et al.,
568 2015; Fell et al., 2011), a method traditionally used to analyze the data with temporal dependencies such
569 as EEG, and has recently been applied to learning functions ^{46,47}. In Experiment 1d, late learning is
570 contaminated by the contribution of aiming strategies. As such, we focused on the aftereffect data,
571 comparing the heading angle in the first cycle of this block with the average heading angle during the no-
572 feedback baseline block.

573

574 In Experiment 3, adaptation was defined as the difference in hand angle between trial $n+1$ and trial n . To
575 construct functions describing how adaptation changed as a function of feedback timing we computed,
576 for each trial, the actual interval between feedback onset time and either movement onset or movement
577 offset. For the movement onset (offset) function, negative and positive values indicate that the feedback
578 preceded or followed movement onset (offset), respectively.

579

580 To quantify the peak in the four adaptation functions (two distances, with one function for movement
581 onset and one for movement offset), we combined the data across trials and participants and fit the data
582 with a skewed-Gaussian function:

583
$$y = 2 * \frac{e^{\frac{-x^2}{2}}}{\sqrt{2\pi}} * CDF_{Gaussian}(\alpha x) * b - c, \quad [1]$$

584
$$x = \frac{t-d}{e}, \quad [2]$$

585 where y is mean Δ hand angle, t is the feedback onset time subtracted by either movement onset or
586 movement offset, and $cdf_{Gaussian}$ is the cumulative distribution of the standard Gaussian distribution.

587 There are five free parameters: a , b , c , d , and e , corresponding to the width, height, lower boundary, shift
588 of the mean from zero, and skewedness of the function. To estimate the variability of each parameter, we
589 performed a jackknife resampling procedure, leaving out the data from one participant and using the
590 remaining data to estimate the function. This procedure was repeated with each participant excluded
591 once.

592

593 To determine the movement trajectory, the radial axis was evenly divided into 150 segments from the
594 initial hand position to the target. We used interpolation to obtain the heading angle for each segment.
595 For Experiment 2, the initial heading angle was calculated by averaging the theta-angular-value at the first
596 30 cut points, and the end angle is defined as the theta-value at the 150th cut-point (target distance).

597

598 Between-condition comparisons were performed with t-tests or ANOVAs, with Bonferroni corrections for
599 multiple comparisons applied when appropriate. For the t-tests, we report the Bayes factor, reflective of
600 the ratio of the likelihood of the alternative hypothesis (H1) over the null hypothesis (H0), and Cohen's d,
601 a measure of effect size. For ANOVAs, the effect size is reported using partial eta squared η_p^2 . In all tests,
602 we confirmed that the data met the assumptions of a Gaussian distribution and homoscedasticity.

603

604 **Data and code availability**

605 Data for this paper and codes for analyses are available at <https://osf.io/ej4ba/>

606

607 **Author contributions**

608 T.W., G.A., J.S.T., R.B.I. contributed to the conceptual development of this project. T.W. and T.T. collected
609 the data. T.W. analyzed the data, prepared the figures, and wrote the initial draft of the paper, with all
610 the authors involved in the editing process.

611

612 **Funding**

613 RBI is funded by the NIH (grants NS116883 and NS105839). JST is funded by the PODS II scholarship from
614 the Foundation for Physical Therapy Research and by the NIH (F31NS120448).

615

616 **Competing interests**

617 RI is a co-founder with equity in Magnetic Tides, Inc.

618 References

619 1. Wolpert, D. M. & Flanagan, J. R. Motor prediction. *Curr. Biol.* **11**, R729–32 (2001).

620 2. Krakauer, J. W., Hadjiosif, A. M., Xu, J., Wong, A. L. & Haith, A. M. Motor Learning. *Compr. Physiol.* **9**,
621 613–663 (2019).

622 3. Kim, H. E., Avraham, G. & Ivry, R. B. The Psychology of Reaching: Action Selection, Movement
623 Implementation, and Sensorimotor Learning. *Annu. Rev. Psychol.* **72**, 61–95 (2021).

624 4. Schween, R., Taube, W., Gollhofer, A. & Leukel, C. Online and post-trial feedback differentially affect
625 implicit adaptation to a visuomotor rotation. *Exp. Brain Res.* **232**, 3007–3013 (2014).

626 5. Hinder, M. R., Tresilian, J. R., Riek, S. & Carson, R. G. The contribution of visual feedback to visuomotor
627 adaptation: how much and when? *Brain Res.* **1197**, 123–134 (2008).

628 6. Barkley, V., Salomonczyk, D., Cressman, E. K. & Henriques, D. Y. P. Reach adaptation and
629 proprioceptive recalibration following terminal visual feedback of the hand. *Front. Hum. Neurosci.* **8**,
630 705 (2014).

631 7. Taylor, J. A., Krakauer, J. W. & Ivry, R. B. Explicit and Implicit Contributions to Learning in a
632 Sensorimotor Adaptation Task. *Journal of Neuroscience* **34**, 3023–3032 (2014).

633 8. Held, R., Efstathiou, A. & Greene, M. Adaptation to displaced and delayed visual feedback from the
634 hand. *J. Exp. Psychol.* **72**, 887–891 (1966).

635 9. Brudner, S. N., Kethidi, N., Graeupner, D., Ivry, R. B. & Taylor, J. A. Delayed feedback during
636 sensorimotor learning selectively disrupts adaptation but not strategy use. *J. Neurophysiol.* **115**,
637 1499–1511 (2016).

638 10. Botzer, L. & Karniel, A. Feedback and feedforward adaptation to visuomotor delay during reaching
639 and slicing movements. *Eur. J. Neurosci.* **38**, 2108–2123 (07/2013).

640 11. Smith, W. M. & Bowen, K. F. The Effects of Delayed and Displaced Visual Feedback on Motor Control.
641 *J. Mot. Behav.* **12**, 91–101 (06/1980).

642 12. Zhou, W., Fitzgerald, J., Colucci-Chang, K., Murthy, K. G. & Joiner, W. M. The temporal stability of
643 visuomotor adaptation generalization. *J. Neurophysiol.* **118**, 2435–2447 (2017).

644 13. Kitazawa, S., Kohno, T. & Uka, T. Effects of delayed visual information on the rate and amount of
645 prism adaptation in the human. *J. Neurosci.* **15**, 7644–7652 (1995).

646 14. Kitazawa, S. & Yin, P.-B. Prism adaptation with delayed visual error signals in the monkey. *Exp. Brain
647 Res.* **144**, 258–261 (2002).

648 15. Sülzenbrück, S. & Heuer, H. Type of visual feedback during practice influences the precision of the
649 acquired internal model of a complex visuo-motor transformation. *Ergonomics* **54**, 34–46 (2011).

650 16. Morehead, J. R., Taylor, J. A., Parvin, D. E. & Ivry, R. B. Characteristics of Implicit Sensorimotor
651 Adaptation Revealed by Task-irrelevant Clamped Feedback. *J. Cogn. Neurosci.* **29**, 1061–1074 (2017).

652 17. Kim, H. E., Morehead, J. R., Parvin, D. E., Moazzezi, R. & Ivry, R. B. Invariant errors reveal limitations
653 in motor correction rather than constraints on error sensitivity. *Commun Biol* **1**, 19 (12/2018).

654 18. Tsay, J. S., Parvin, D. E. & Ivry, R. B. Continuous reports of sensed hand position during sensorimotor
655 adaptation. *J. Neurophysiol.* **124**, 1122–1130 (2020).

656 19. Tsay, J. S., Ivry, R. B., Lee, A. & Avraham, G. Moving outside the lab: The viability of conducting
657 sensorimotor learning studies online. *Neurons, Behavior, Data analysis, and Theory* (2021)
658 doi:10.51628/001c.26985.

659 20. Anwyl-Irvine, A. L., Dalmaijer, E. S., Hodges, N. & Evershed, J. *Online Timing Accuracy and Precision:
660 A comparison of platforms, browsers, and participant's devices*. <https://osf.io/jfeca> (2020).

661 21. Bond, K. M. & Taylor, J. A. Flexible explicit but rigid implicit learning in a visuomotor adaptation task.
662 *J. Neurophysiol.* **113**, 3836–3849 (06/2015).

663 22. Tsay, J. S. *et al.* The effect of visual uncertainty on implicit motor adaptation. *J. Neurophysiol.* **125**,
664 12–22 (2021).

665 23. Maresch, J., Werner, S. & Donchin, O. Methods matter: Your measures of explicit and implicit
666 processes in visuomotor adaptation affect your results. *Eur. J. Neurosci.* **53**, 504–518 (01/2021).

667 24. Nowak, L. G. & Bullier, J. The Timing of Information Transfer in the Visual System. in *Extrastriate*
668 *Cortex in Primates* (eds. Rockland, K. S., Kaas, J. H. & Peters, A.) 205–241 (Springer US, 1997).

669 25. Thoroughman, K. A., Fine, M. S. & Taylor, J. A. Trial-by-trial motor adaptation: a window into
670 elemental neural computation. *Prog. Brain Res.* **165**, 373–382 (2007).

671 26. Batcho, C. S., Gagné, M., Bouyer, L. J., Roy, J. S. & Mercier, C. Impact of online visual feedback on
672 motor acquisition and retention when learning to reach in a force field. *Neuroscience* **337**, 267–275
673 (2016).

674 27. Wagner, M. J. & Smith, M. A. Shared internal models for feedforward and feedback control. *J.*
675 *Neurosci.* **28**, 10663–10673 (2008).

676 28. Schwein, R. & Hegele, M. Feedback delay attenuates implicit but facilitates explicit adjustments to a
677 visuomotor rotation. *Neurobiol. Learn. Mem.* **140**, 124–133 (04/2017).

678 29. Debats, N. B. & Heuer, H. Exploring the time window for causal inference and the multisensory
679 integration of actions and their visual effects. *R. Soc. open sci.* **7**, 192056 (08/2020).

680 30. Tsay, J. S., Kim, H., Haith, A. M. & Ivry, R. B. Understanding implicit sensorimotor adaptation as a
681 process of proprioceptive re-alignment. *Elife* **11**, e76639 (2022).

682 31. Fetz, E. E., Finocchio, D. V., Baker, M. A. & Soso, M. J. Sensory and motor responses of precentral
683 cortex cells during comparable passive and active joint movements. *J. Neurophysiol.* **43**, 1070–1089
684 (1980).

685 32. Flanders, M. & Cordo, P. J. Kinesthetic and visual control of a bimanual task: specification of direction
686 and amplitude. *J. Neurosci.* **9**, 447–453 (1989).

687 33. Raymond, J. L., Lisberger, S. G. & Mauk, M. D. The cerebellum: a neuronal learning machine? *Science*
688 **272**, 1126–1131 (1996).

689 34. Yeo, C. H., Hardiman, M. J. & Glickstein, M. Classical conditioning of the nictitating membrane
690 response of the rabbit. I. Lesions of the cerebellar nuclei. *Exp. Brain Res.* **60**, 87–98 (1985).

691 35. Smith, M. C., Coleman, S. R. & Gormezano, I. Classical conditioning of the rabbit's nictitating
692 membrane response at backward, simultaneous, and forward CS-US intervals. *J. Comp. Physiol.*
693 *Psychol.* **69**, 226–231 (1969).

694 36. Schneiderman, N. & Gormezano, I. Conditioning of the nictitating membrane of the rabbit as a
695 function of cs-us interval. *J. Comp. Physiol. Psychol.* **57**, 188–195 (1964).

696 37. Frey, P. W. & Ross, L. E. Rabbit eyelid conditioning: Effects of age, interstimulus interval, and intertrial
697 interval. *Dev. Psychobiol.* **1**, 276–279 (1968).

698 38. Smith, M. C. CS-US interval and US intensity in classical conditioning of the rabbit's nictitating
699 membrane response. *J. Comp. Physiol. Psychol.* **66**, 679–687 (1968).

700 39. Avraham, G., Taylor, J. A., Breska, A., Ivry, R. B. & McDougle, S. D. Contextual effects in sensorimotor
701 adaptation adhere to associative learning rules. *bioRxiv* (2020) doi:10.1101/2020.09.14.297143.

702 40. Kim, O. A., Forrence, A. D. & McDougle, S. D. Motor learning without movement. *Proc. Natl. Acad.*
703 *Sci. U. S. A.* **119**, e2204379119 (2022).

704 41. Magill, R. & Anderson, D. Motor learning and control.
705 https://www.academia.edu/download/62953224/Motor_Learning_and_Control__Concepts_and_-
706 [Anderson_David20200414-28877-18hp4j2.pdf](https://www.academia.edu/download/62953224/Motor_Learning_and_Control__Concepts_and_-Anderson_David20200414-28877-18hp4j2.pdf) (2010).

707 42. Schmidt, R. A. & Wrisberg, C. A. *Motor Learning and Performance: A Situation-based Learning*
708 *Approach*. (Human Kinetics, 2008).

709 43. Oldfield, R. C. The assessment and analysis of handedness: The Edinburgh inventory.
710 *Neuropsychologia* **9**, 97–113 (3/1971).

711 44. McDougle, S. D. & Taylor, J. A. Dissociable cognitive strategies for sensorimotor learning. *Nat.*
712 *Commun.* **10**, 40 (12/2019).

713 45. Botzer, L. & Karniel, A. A Simple and Accurate onset Detection Method for a Measured Bell-shaped

714 Speed Profile. *Front. Neurosci.* **3**, 61 (2009).

715 46. Avraham, G., Morehead, J. R., Kim, H. E. & Ivry, R. B. Reexposure to a sensorimotor perturbation

716 produces opposite effects on explicit and implicit learning processes. *PLoS Biol.* **19**, e3001147 (2021).

717 47. Labruna, L. *et al.* Individual differences in TMS sensitivity influence the efficacy of tDCS in facilitating

718 sensorimotor adaptation. *Brain Stimul.* **12**, 992–1000 (2019).

719 **Supplementary Material**

720 **Supplementary Methods**

721 *Power analysis.* We are interested in what is the key factor that caused the difference in implicit
722 adaptation between the endpoint and the continuous feedback. For the block design experiments (Exp 1-
723 2), we computed minimum sample sizes based on the no-feedback washout block from Taylor, Krakauer,
724 Ivry (2014) in a study that used endpoint and continuous feedback. We estimated the power for an
725 independent samples t-test using a two-tailed test with significance set at 0.05 and a power of 0.9. The
726 effect size was $d=0.91$ (continuous feedback group had a mean of 25.9° S.D. of 4.9° ; endpoint feedback
727 group had a mean of 21.6° and S.D. of 4.1°), indicating a minimum sample size of 27 participants for each
728 condition. Given our experience that some participants perform poorly (e.g., fail to pay attention) on web-
729 based experiment (see details in the next section), we decided to recruit 25% more participants than the
730 size suggested by the power analyses, resulting in a target of 34 participants for each feedback condition.
731 Half experienced a clockwise perturbation and the other half a counter-clockwise perturbation. For the 2°
732 clamp task (Exp. 1c), we recruited 28 participants for each condition with 14 people in each perturbation
733 direction. For Experiment 3, we used a sample size (12 for each condition) that is typical in sensorimotor
734 learning experiments.

735

736 *Outlier removal.* To minimize online corrections, we instructed the participant to move quickly. We
737 excluded trials with a movement time longer than 500 ms. We also excluded trials in which the hand angle
738 at the end of the movement was more than 70° from the target, under the assumption that the participant
739 moved to the wrong target on these trials. If the total number of excluded trials was greater than 30%
740 (movement time and direction), the entire data set for that participant was not included in the analyses.
741 These participants either ignored the instruction to move fast or tended to repeatedly move to the same
742 location, independent of the target location.

743

744 Table S1 Summary of participants' information on web-based experiments.

	<u>Exp1b</u>			<u>Exp1d</u>		<u>Exp2a</u>		<u>Exp2b</u>
	Continuous	Standard-Endpoint	Early-endpoint	Endpoint	Early-endpoint	Extend endpoint	Extend early-endpoint	Advance continuous
Participants meeting inclusion criteria	31	31	28	30	27	32	30	30
Female	19	9	7	13	11	14	13	17
Age (mean (SD))	24.8(5.4)	24.4(5.1)	23.0(4.7)	25.9(4.7)	23.8(4.4)	23.0(3.5)	25.1(4.8)	24.2(4.5)
CCW	14	16	14	17	14	15	17	15

745

	<u>Exp1b</u>			<u>Exp1c</u>		
	Continuous	Standard-Endpoint	Early-endpoint	Continuous	Early-endpoint	Advance continuous
Participants meeting inclusion criteria	28	34	31	27	25	24
Female	12	22	6	18	14	14
Age (mean (SD))	25.3(5.1)	24.8(5.7)	25.3(4.5)	24.1(4.0)	26.3(5.3)	29.3(8.3)
CCW	13	17	15	13	13	14

746

747

748 **Supplementary Results**

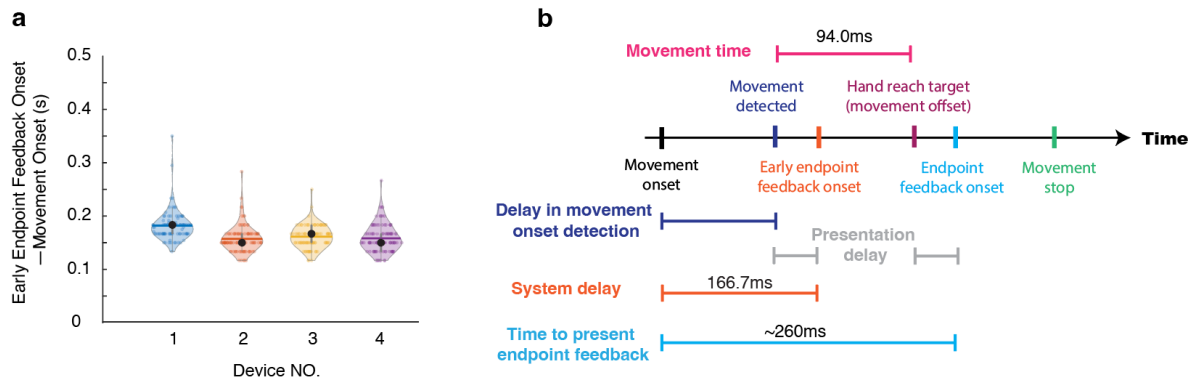
749 There are substantial delays with a web-based experimental system. One delay is introduced by the time
750 required to detect movement along a trackpad, essential for determining movement onset. A second
751 delay is introduced by the time required to present the stimulus (feedback) on the monitor after the
752 command is made by the code. To quantify these delays, we used a camera (frame rate = 60 Hz) to
753 simultaneously record the monitor and movement when participants performed the web-based
754 experiment. We performed these recordings on different devices and, for each setup, measured from the

755 video recordings the delay between movement onset time and feedback onset time (with the program
756 set to present feedback as soon as movement onset was detected, the early-endpoint condition). On
757 average, the delay was 166.7 ms (Fig. S1). Note that in our setup, we cannot partition this value into that
758 associated with movement onset detection and presentation delay. However, a previous study showed
759 that, across devices, the delay to present visual feedback on web-based platforms is around 11.5 (± 15.4)
760 ms²⁰; as such, the majority of the delay in our system is likely due to a delay in detecting movement onset
761 from a trackpad.

762
763 A 166.7 ms system delay in the web-based experiments would suggest that what we refer to as 'early-
764 endpoint feedback' is actually occurring well into the movement. Indeed, this value is close to the peak of
765 the motor correction function measured in the lab-based experiment (Exp. 3). Since movement 'offset',
766 defined as the time when hand reached the target distance, is in the middle of the movement, the time
767 at which movement offset is detected is not influenced by the delay in detecting movement onset.
768 Assuming that the presentation delay for the early-endpoint feedback and the standard-endpoint
769 feedback is the same, standard-endpoint feedback was presented around 94 ms (movement duration)
770 after early-endpoint feedback, or around 260 ms (94+166ms) after movement onset. Therefore, the
771 results showing early-endpoint feedback induced greater adaptation compared to standard-endpoint
772 feedback is consistent with the motor correction function measured in the lab-based experiments.

773
774 There is also a delay between the time when the computer issues a command (e.g., 'draw endpoint
775 feedback) and the time at which the stimulus appears on the screen. For the lab-based experiment,
776 Psychtoolbox adjust this for this when providing information on when the stimulus appears on the
777 monitor. As such, we assume system delays are negligible in Experiment 3.

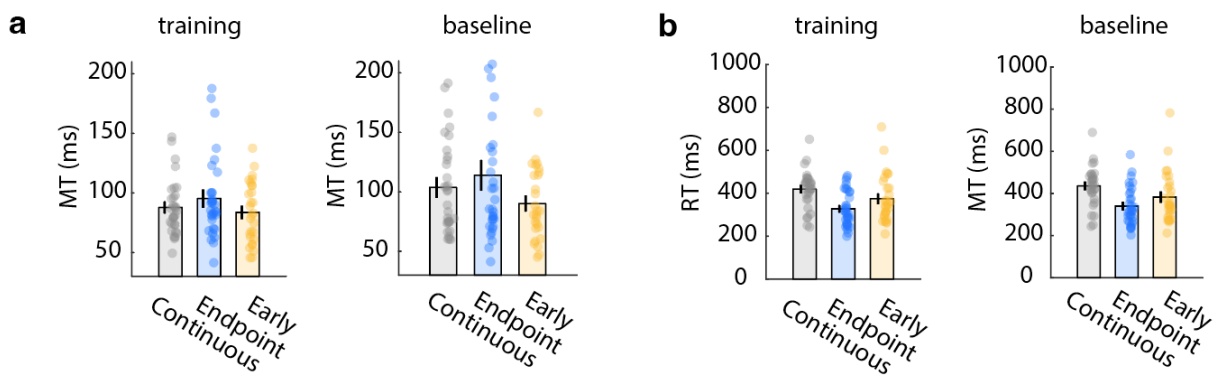
778



779

780 **Figure S1. Delays in our web-based experimental system.** **a**, Average system delays based on video measurements
 781 obtained when running web-based protocol on four devices (1, ThinkPad X1, 2021; 2, hp pavilion 15z-eh000; 3,
 782 MacBook Pro 2020; 4, Dell Xps 13 9365). Videos were examined and manually marked to identify the first frame in
 783 which the hand moved and the first frame in which the feedback cursor was detected. We measured 100 trials for
 784 each device. Each colored dot represents a trial. Black dots indicate the group median and the horizontal lines
 785 indicate the group means (182.2, 157.2, 161.3, 158.2 ms for devices 1-4 respectively). **b**, Timeline of the web-based
 786 experiment. The early-endpoint feedback is presented approximately 166.7 ms after movement onset. This value
 787 includes delays associated with movement onset detection and feedback presentation. The temporal difference
 788 between the standard endpoint feedback and the early endpoint feedback should be equal to movement duration.
 789 From this, we can infer that endpoint feedback is presented, on average, 260 ms after movement onset.

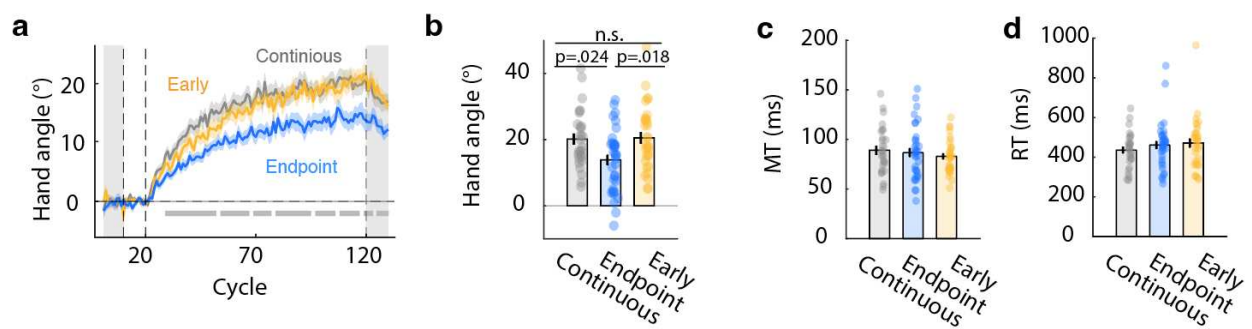
790



791

792 **Figure S2.** Movement duration (a) and reaction time (b) for Experiment 1. The endpoint group had longer movement
793 times and faster reaction times compared with the other two groups. These differences are observed in both the
794 adaptation and baseline blocks. Given that the task was identical for all three groups in the baseline block, the
795 differences here presumably reflect random variation in our three samples and do not result from the feedback
796 manipulation. Note that, given the delay in detecting movement onset, the values reported here overestimate
797 reaction time and underestimate movement time.

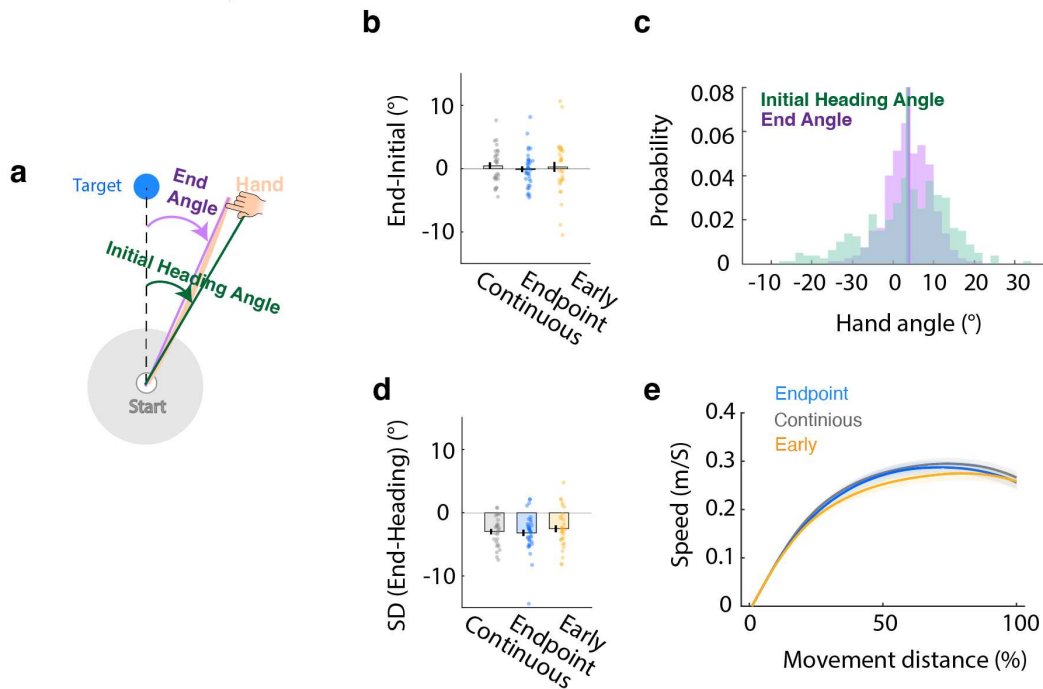
798



799

800 **Figure S3.** Results from Experiment 1b. Replication of Experiment 1 that includes measurement of the full trajectory.
801 (a) Time course of hand angle. The shaded area represents standard error. The light gray areas indicate the baseline
802 and washout blocks. Horizontal grey lines at the button indicate results of cluster-based ANOVA. Similar to the results
803 of Experiment 1a, early-endpoint feedback induced larger adaptation compared to standard-endpoint feedback. No
804 difference was observed between the early-endpoint and continuous feedback conditions. (b) Late adaptation. Error
805 bars indicate standard error and dots represent each participant. n.s., non-significant. (c) Movement time is
806 comparable across conditions (86.2 ± 23.1 ms; $F(2, 90)=0.68$, $p=0.51$, $BF_{10}=0.07$, $\eta_p^2=0.01$). (d) Reaction time is
807 comparable across conditions (457.2 ± 114.8 ms; $F(2, 90)=0.71$, $p=0.49$, $BF_{10}=0.07$, $\eta_p^2=0.01$).

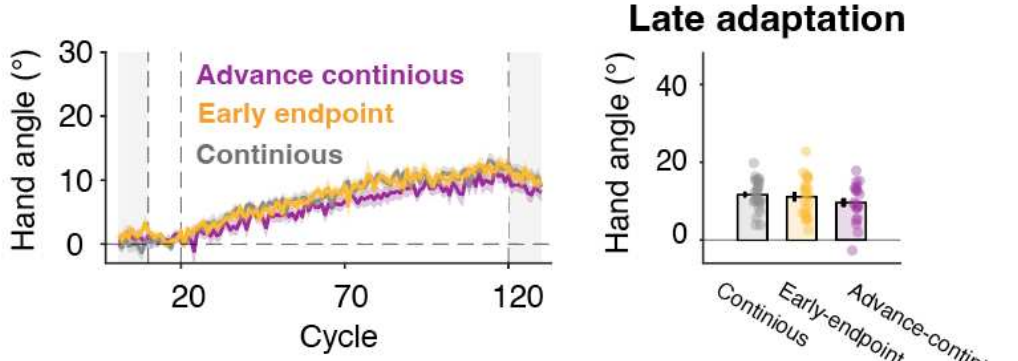
808



809

810 **Figure S4.** Movement kinematics were not influenced by feedback format. (a) Illustration of the definition of initial
811 heading angle and end angle of the movement. (b) Change between initial heading angle and final heading angle.
812 Positive values indicate angle of hand at target amplitude is larger than initial measurement of hand angle, the
813 direction expected if participants were making an on-line correction. The heading angle remained relatively constant
814 across the movement in all three conditions. Error bar indicates standard error and each dot the value for a
815 participant. (c) Distribution of the initial and end heading angles for a typical participant. The initial heading angle is
816 nosier than the end angle. (d) Difference in standard deviation of the initial and end heading angles. The latter is
817 smaller in all three conditions. This effect is likely due to variation in the exact position of the hand within the start
818 circle. Given the difference in variance and absence of evidence of online corrections, we opted to use the end angle
819 as the primary dependent variable. (e) Normalized mean speed profile for the three feedback conditions.

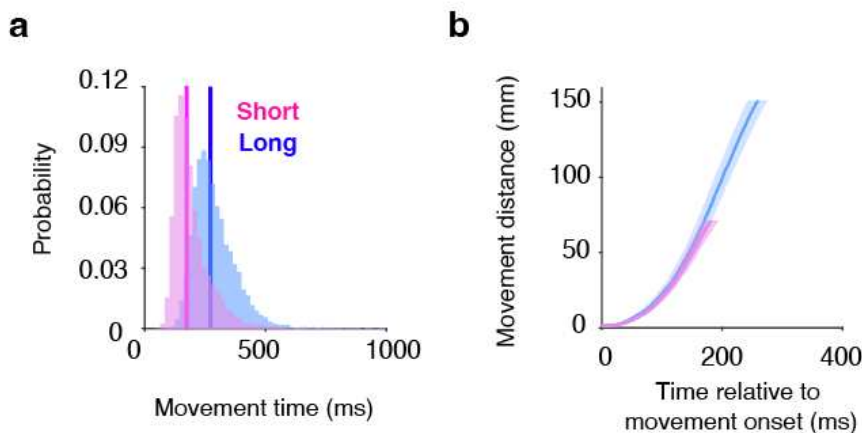
820



821

822 **Figure S5.** Results from Experiment 1c in which the clamp size was reduced to 2°. Adaptation was similar in response
823 to early-endpoint, continuous, and advanced-continuous feedback conditions. Left: Time course of hand angle. The
824 shaded area indicates standard error. No significant differences were found in the cluster-based ANOVA. Right: Hand
825 angle in late adaptation. Error bar indicates standard error and each dot a participant.

826

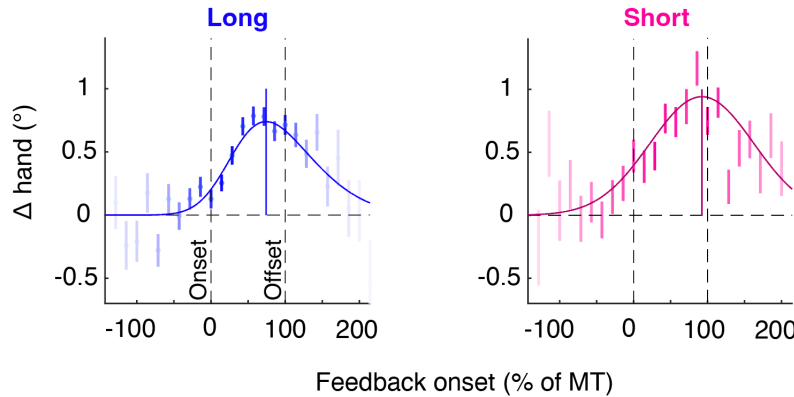


827

828 **Figure S6.** Increasing movement distance was effective manipulation for increasing movement duration in
829 Experiment 3. **a**, Movement duration distributions for the short and long conditions. Thick vertical lines indicate
830 group medians. **b**, Average hand distance as a function of time, relative to movement onset.

831

832



833

834 **Figure S7.** Trial-by-trial motor correction plotted as a function of feedback of normalized movement time (based on
 835 when hand reached target amplitude). The feedback onset time for each trial was aligned with movement onset and
 836 then divided by the movement duration of that trial. Bin size is 15% and the darkness of the dot indicates the relative
 837 number of samples in each bin. Colored curve indicates the best-fitted skewed Gaussian, with the colored vertical
 838 line marking the peak of the function.

839

840 Table S2: Linear regression results for Experiment 1

	Coefficient (mean (SE))	T value	P value
Intercept	15.7(5.4)	2.9	0.005
Early-endpoint¹	6.1(2.5)	2.5	0.016
Continuous¹	5.4(2.5)	2.1	0.036
Age	0.007(0.2)	0.03	0.98
Gender²	-2.3(2.3)	-1.0	0.32
Perturbation direction³	-0.67(2.0)	-0.34	0.73
Movement time	0.45(1.1)	0.43	0.67
Reaction time	2.6(1.3)	1.9	0.053

841 ¹, feedback type is a categorical variable with the endpoint feedback as the baseline condition

842 ², gender is a categorical variable with male as the baseline condition

843 ³, Perturbation is a categorical variable with CCW as the baseline condition